UNIVERSIDADE ESTADUAL DE CAMPINAS
SISTEMA DE BIBLIOTECAS DA UNICAMP
REPOSITÓRIO DA PRODUÇÃO CIENTIFICA E INTELECTUAL DA UNICAMP

Versão do arquivo anexado / Version of attached file:

Versão do Editor / Published Version

Mais informações no site da editora / Further information on publisher's website:

https://www.nature.com/articles/srep06252

DOI: 10.1038/srep06252

Direitos autorais / Publisher's copyright statement:

SCIENTIFIC REPORTS

OPEN

Possible unconventional superconductivity in substituted BaFe$_2$As$_2$ revealed by magnetic pair-breaking studies

P. F. S. Rosa[1,2], C. Adriano[1], T. M. Garitezi[1], M. M. Piva[1,4], K. Mydeen[4], T. Grant[2], Z. Fisk[2], M. Nicklas[4], R. R. Urbano[1], R. M. Fernandes[3] & P. G. Pagliuso[1]

[1]Instituto de Física "Gleb Wataghin", UNICAMP, Campinas-SP, 13083-859, Brazil, [2]University of California, Irvine, California 92697-4574, USA, [3]School of Physics and Astronomy, University of Minnesota, Minneapolis, MN 55455, USA, [4]Max Planck Institute for Chemical Physics of Solids, Nöthnitzer Str. 40, D-01187 Dresden, Germany.

The possible existence of a sign-changing gap symmetry in BaFe$_2$As$_2$-derived superconductors (SC) has been an exciting topic of research in the last few years. To further investigate this subject we combine Electron Spin Resonance (ESR) and pressure-dependent transport measurements to investigate magnetic pair-breaking effects on BaFe$_{1.9}$M$_{0.1}$As$_2$ (M = Mn, Co, Cu, and Ni) single crystals. An ESR signal, indicative of the presence of localized magnetic moments, is observed only for M = Cu and Mn compounds, which display very low SC transition temperature (T_c) and no SC, respectively. From the ESR analysis assuming the absence of bottleneck effects, the microscopic parameters are extracted to show that this reduction of T_c cannot be accounted by the Abrikosov-Gorkov pair-breaking expression for a sign-preserving gap function. Our results reveal an unconventional spin- and pressure-dependent pair-breaking effect and impose strong constraints on the pairing symmetry of these materials.

The Fe-based superconductors (SC) RFeAsO (R = La-Gd) and AFe$_2$As$_2$ (A = Ba, Sr, Ca, Eu) have been a topic of intense scientific investigation since their discovery[1,2]. In particular, the semi-metal member BaFe$_2$As$_2$ (Ba122) displays a spin-density wave (SDW) phase transition at 139 K which can be suppressed by hydrostatic pressure and/or chemical substitution (e.g. K, Co, Ni, Cu, and Ru) inducing a SC phase[3,40,60–62]. Although the proximity to a SDW state suggests a magnetic-mediated pairing mechanism[4,5], the precise nature and symmetry of the SC state, as well as the microscopic mechanism responsible for driving the SDW phase towards a SC state, remain open questions begging for further investigation. Importantly, suppressing the SDW phase – either via applied pressure or chemical substitution – is not sufficient for SC to emerge[16,20]. Furthermore, when SC is found, the achieved optimal T_c differs dramatically depending on the particular chemical substitution. This difference may be related to the pair-breaking effect associated with substitutions, which create local impurity scatterers, particularly when introduced in the FeAs planes[21].

A complete understanding of the impurity pair-breaking (IPB) effect in the Fe-pnictides is hindered, however, by their multi-band character and by the absence of quantitative information about the impurity potential[4]. Indeed, the suppression of T_c by impurities has been used as an argument in favor of both a sign-preserving s^{++} state[22,23] and a sign-changing s^{+-} state in Ba122-derived materials[24–26]. In these analyses, the impurity potential is usually estimated by the changes in the residual resistivity. However, the latter is sensitive to the transport scattering rate, which may differ from the quasi-particle scattering rate related to the suppression of T_c. Furthermore, using optimally-doped (OPD) compositions to study the effects of impurities on T_c may introduce additional complications, since any kind of perturbation will likely drive the system away from the vicinity of the SDW phase and suppress SC by diminishing the strength of the pairing interaction instead of breaking the Cooper pairs[23,27].

In this paper, we circumvent these issues by combining macro and microscopic experiments, namely pressure-dependent transport measurements and electron spin resonance (ESR) in order to investigate the magnetic IPB effects in BaFe$_{1.9}$M$_{0.1}$As$_2$ (M = Mn, Co, Cu, and Ni) single crystals slightly below the OPD concentration. A sizeable ESR signal for M = Mn, Cu samples provides not only direct evidence for their role as local magnetic impurities, but it also allows us to extract the averaged exchange coupling $\langle J^2(\mathbf{q})\rangle$ between them and the Fe 3d

conduction electrons. The estimated suppression of T_c derived from this quantity, which plays the role of the magnetic impurity potential in the Abrikosov-Gor'kov (AG) formalism[29,30], is found to be significantly smaller than the observed one, in sharp contrast to the excellent agreement found previously in borocarbides[31,37,38] – multi-band compounds that display conventional sign-preserving SC states. Furthermore, we find that pressure strongly enhances T_c of the M = Cu sample, presumably by promoting stronger Cu–Fe hybridization and consequently suppressing the IPB effect. Our findings impose strong constraints on the mechanism responsible for SC and provide a strong evidence for an unconventional gap symmetry in these materials.

Fig. 1 displays the in-plane electrical resistivity, $\rho_{ab}(T)$, at ambient pressure for the selected single crystals. A linear metallic behavior is observed at high-T and the SDW phase transition of the parent compound is suppressed for all substitutions. A slight upturn is still present (arrows in Fig. 1), as typically found for substituted samples of Ba122 slightly below the OPD concentration[3]. As T is further decreased, SC emerges with the onset of T_c, defined as the temperature at which $d\rho_{ab}/dT = 0$, at 26.1 K, 22.2 K, and 3.8 K for Co, Ni, and Cu substitutions, respectively. On the other hand, no T_c is observed for M = Mn.

Figs. 2a–b show $\rho_{ab}(T)$ as a function of pressure for Co and Ni-substituted compounds. A small increase of T_c is observed, as expected for nearly OPD samples[3]. For instance, T_c reaches 28.6 K at 18 kbar for M = Co, whereas the self-flux OPD compound reaches a maximum T_c of $\sim$23 K in the same pressure range, suggesting that the In-flux samples are of high quality. On the other hand, for M = Ni, T_c only reaches 24.7 K. One can speculate that the reason the Ni-OPD sample does not achieve $T_c \sim$ 29 K is that it introduces more disorder than cobalt[8–10]. Indeed, the residual resistivity is higher for M = Ni. Furthermore, the highest T_c found in FeAs-based SC is obtained through out-of-plane substitution[41,42].

Now we turn our attention to the striking behavior of Mn- and Cu-substituted compounds, shown in Figs. 2c–d. First, we observe a substantial unexpected enhancement of T_c by a factor of $\sim$2.5 (T_c = 10 K at 24 kbar) for the Cu-substituted compound. Although an increase of T_c is expected for underdoped samples[17–19], the maximum T_c achieved is also expected to be roughly the same as in the OPD sample at ambient pressure. Surprisingly, this is not the case for the studied Cu-substituted compound, which presents T_c = 4.2 K for the OPD crystal. On the other hand, SC does not emerge for M = Mn up to P = 25 kbar, in agreement with previous reports[16]. In addition, there is a drastic decrease of $\rho_{ab}(T)$ with pressure by a factor of $\sim$3 for M = Cu and of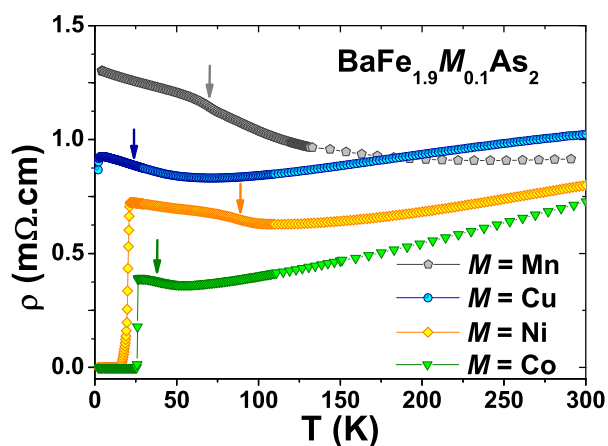 $\sim$1.5 for M = Mn over all T range (see Fig. 1 for a comparison), suggesting a possible decrease of the impurity scattering potential. These results seem to be consistent with a magnetic IPB mechanism since – unlike their Co and Ni counterparts – Mn and Cu substitutions are expected to introduce local moments. In many compounds, pressure is well known to enhance the hybridization between the local moments and the conduction electrons[43–47]. Such enhancement would suppress the magnetic IPB effect and, consequently, increase T_c. As Mn^{2+} has a much higher spin (S = 5/2) than Cu^{2+} (S = 1/2), it is not surprising that the magnetic IPB is larger for M = Mn, which in turn does not display SC.

To investigate such magnetic IPB scenario, we performed ESR – a powerful spin probe technique sensitive to the presence of local moments and their coupling to the conduction electrons[48]. In agreement with the expectation that Cu and Mn ions have local moments, our ESR data reveal an intense resonance line for M = Cu and Mn, but not for M = Co and Ni. Fig. 3 shows the X-Band ESR lines normalized by the concentration of paramagnetic ions at T = 150 K for fine powders of gently crushed single crystals. The Lorentzian fitting of the spectra reveals a linewidth of ΔH = 600(60) G and a g-value of g = 2.08(3) for M = Cu. For M = Mn, g = 2.04(3) and the linewidth is slightly larger, ΔH = 750(80) G, indicating stronger Mn-Mn interactions. Finally, for M = Mn and Co, g = 2.05(3) and ΔH = 670(70) G. For all samples, the calibrated number of resonating spins at room-T is in good agreement with the concentrations obtained from Energy Dispersive Spectroscopy (EDS). As expected, the ESR intensity, which is proportional to $S(S + 1)$, was found to be roughly twelve times larger for M = Mn samples, as compared to the M = Cu sample. These results also indicate that the oxidation states of Cu and Mn are indeed Cu^{2+} (S = 1/2) and Mn^{2+} (S = 5/2). In the former case, Cu^{+} ($3d^{10}$ state) would not display an ESR resonance line since it is not a paramagnetic ion. In the case of copper, Cu^{+} ($3d^{10}$ state) would not display an ESR resonance line since it is not a paramagnetic probe with unpaired electrons. In the case of manganese, for Mn^{3+} (S = 2) and Mn^{4+} (S = 3/2) ions, one would expect a distinct ESR response (i.e., different g-value and calibrated signal intensity). Consequently, one can infer that there is no effective charge doping into the system, as suggested previously both experimentally and theoretically[6,8]. Furthermore, our ESR results agree with other indirect probes that also suggest localized Cu^{2+} and Mn^{2+} moments in chemically-substituted Ba122[49–53]. We note that the detailed analysis of the ESR data confronted with Eu-substituted $BaFe_{2−x}M_xAs_2$ (M = Co, Ni, Cu, Mn, and Ru) requires further technical discussion. Therefore, it will be the focus of a separated report[13,15].

Besides revealing the presence of localized moments, ESR also allows us to extract the averaged squared exchange coupling $\langle J^2(\mathbf{q})\rangle$ between the localized moments and the conduction electrons from the linear increase of the linewidth with temperature (Korringa behavior) (see Table I)[12,13,15,31,37,38]. In a general approach for single-band metals, the thermal broadening b of the ESR linewidth $\Delta H \simeq 1/T_1$ is the linear well-known Korringa relaxation defined as $b \equiv \dfrac{d(\Delta H)}{dT} = \dfrac{\pi k_B}{g\mu_B}\left\langle J_{fs}^2(\mathbf{q})\right\rangle \eta^2(E_F)\dfrac{K(\alpha)}{(1-\alpha)^2}$[32]. Here, $\langle J_{fs}(\mathbf{q})^2\rangle^{1/2}$ is the effective exchange interaction between the local moment and the conduction electrons (ce) in the presence of ce momentum transfer averaged over the whole Fermi surface (FS)[34], $\eta(E_F)$ is the "bare" density of states (DOS) for one spin direction at the Fermi level, g is the local moment g-value and $K(\alpha)$ is the Korringa exchange enhancement factor due to electron-electron exchange interaction[35,36]. In the present analysis, we found empirically that "bottleneck" and "dynamic" effects are not present[33]. When "dynamic" effects are present the g-values are usually strongly T-dependent, which is not observed in our experimental data. Moreover, when "bottleneck" effects are relevant the Korringa rate b decreases with increasing concentration of the magnetic ions. However, in our data, we observe that spin-spin interaction dominates the entire temper-
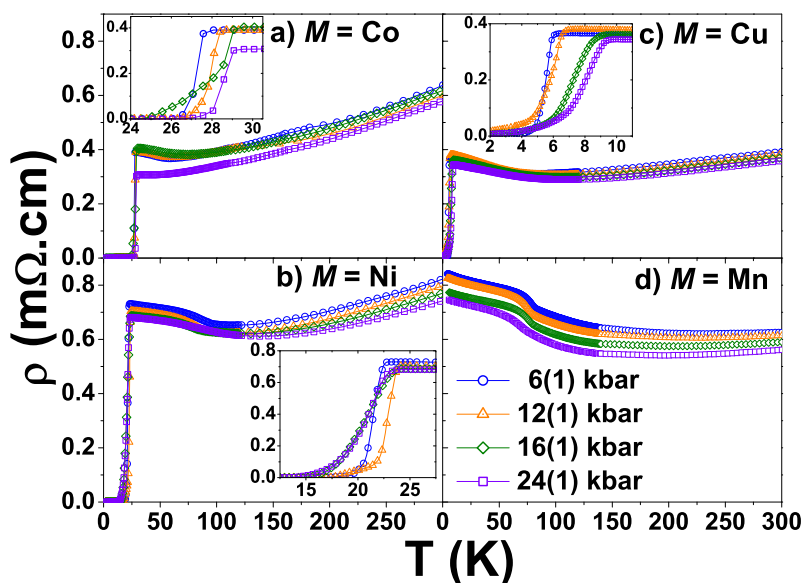

Figure 1 | In-plane electrical resistivity, $\rho_{ab}(T)$, for $BaFe_{1.9}M_{0.1}As_2$ (M = Mn, Cu, Ni, Co) single crystals. The arrows show the minima of the first derivative in the vicinity of the SDW transition.

Figure 2 | $\rho_{ab}(T)$ vs. T for BaFe$_{1.9}$$M_{0.1}As_2$ (M = Co, Cu, Ni, and Mn) single crystals for P = 5–25 kbar. The insets show the evolution of T_c with pressure.

ature range for dilute concentrations of Mn and Cu ions. In addition, bottleneck effects are not observed in Eu-substituted BaFe$_2$As$_2$[12], indicating that FeAs-based compounds are intrinsically unbottle-necked systems likely due to fast relaxation rates between the 3d conduction electrons and the lattice. In fact, recent ultrafast spectroscopy measurements have found a very large spin-lattice coupling in BaFe$_2$As$_2$[28]. Finally, even if bottleneck effects were present, they alone would hardly be able to account for the enormous difference between J_{ESR} and J_{AG} observed here.

The key point here is that this parameter $\langle J^2(\mathbf{q})\rangle$ is the same one determining the suppression of T_c by magnetic impurities within the AG formalism[29,30]. To estimate whether the extracted value of $\langle J^2(\mathbf{q})\rangle_{ESR}$ for M = Cu and Mn compounds can account for the observed suppression of T_c in this formalism, we consider the "con-

ventional case", where the gap function has the same amplitude and sign across the entire Brillouin zone. This is the scenario in which magnetic impurities have the strongest effect on T_c – in fact, introducing anisotropies in the gap function would make the magnetic pair-breaking effect weaker[54,55]. In this situation, we have[30]:

$$\ln\left(\frac{T_{c,0}}{T_c}\right) = \psi\left(\frac{1}{2} + \frac{1}{2\pi T_c \tau_s}\right) - \psi\left(\frac{1}{2}\right), \quad (1)$$

where $\psi(x)$ is the digamma function, $T_{c,0}$ is the transition temperature in the absence of magnetic impurities, and $\tau_s^{-1} = \frac{\pi}{2}\Delta c\eta(E_F)$ $\langle J^2(\mathbf{q})\rangle S(S+1)$ is the magnetic scattering rate. Here, $\eta(E_F)$ is the density of states per spin at the Fermi level, Δc is the magnetic impurity concentration, and S, the spin of the localized moment. Given that $\Delta c < 0.1$ in our samples, we can perform a series expansion of eq. 1 and obtain the simplified expression:

$$\left|\frac{\Delta T_c}{\Delta c}\right| = \frac{\pi^2}{8}\eta(E_F)\langle J^2(\mathbf{q})\rangle S(S+1), \quad (2)$$

with $\Delta T_c = T_c - T_{c,0}$. The value for $\eta(E_F)$ is extracted from the linear coefficient of the low-temperature specific heat γ, yielding $\eta(E_F)$ = 3.34 states/eV.spin.FU for one mole, which is the same for all compounds[2,13]. Small variations of γ across different compositions would not alter our main conclusions, as we discuss below. Moreover, the nearly constant ESR g-shift value found for the various ESR probes as a function of different chemical substitutions in Ba122 compounds is a strong evidence that the density of states at the Fermi level is nearly the same for pure Ba122 and for all studied compounds[13]. The choice of $T_{c,0}$ = 26 K is a more subtle issue. Since the dependence of T_{SDW} with x in the phase diagrams of the BaFe$_{2-x}$$M_xAs_2$ compounds is nearly identical for M = Co, Ni, Cu[27], if one assumes that superconductivity is governed by fluctuations associated with the normal state, then one would expect that the optimal T_c values of these three samples would be very similar. Indeed, this is the case for M = Co and Ni, which also display similar maximum values of T_c under pressure. However, for M = Cu the value of T_c is significantly smaller – but this sample displays an ESR signal, unlike M = Co and Ni. We therefore assume that $T_{c,0}$ of the M = Cu sample, and also of the M = Mn sample, is approximately the same as the T_c value of the optimally doped M = Co and Ni samples, where magnetic pair-breaking is absent, according to our ESR analysis. Moreover,
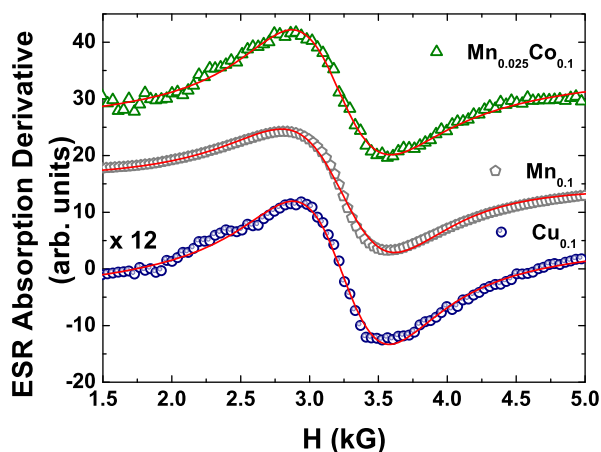

Figure 3 | X-Band ESR lines at T = 150 K for powdered crystals of BaFe$_{1.9}$$M_{0.1}As_2$ (M = Cu, Mn) and BaFe$_{1.895}$Mn$_{0.005}$Co$_{0.1}$As$_2$. The spectra were normalized by the concentration of paramagnetic probes in order to clearly compare their intensities. The solid lines are Lorentzian fits to the spectra (sample grain size smaller than the skin depth[48]). It is worth mentioning that, in order to obtain the ESR signal, the sample surface must be completely clean and free of In-flux. The ESR signals for both samples were calibrated at 300 K using a strong pitch standard sample with 4.55 × 10^{15} spins/cm.

Table I | Experimental and calculated parameters for BaFe$_{1-x}$M$_x$As$_2$ (this work) and conventional SC (refs. [31, 37])

Sample	c (%)	g_{ESR}	$\left|\Delta T_c^{exp}\right|$(K)	$T_{c,0}$ (K)	$\langle J^2(\mathbf{q})\rangle_{ESR}^{1/2}$(meV)	$\langle J^2(\mathbf{q})\rangle_{AG}^{1/2}$(meV)
BaFe$_{1.9}$Cu$_{0.1}$As$_2$	5	2.08(3)	22	26	1.2(5)	111(10)
BaFe$_{1.88}$Mn$_{0.12}$As$_2$	6	2.05(2)	$\geq$26	26	0.7(5)	$\geq$32(3)
BaFe$_{1.895}$Co$_{0.100}$Mn$_{0.005}$As$_2$	0.25	2.06(2)	10	26	0.8(5)	98(9)
Lu$_{1-x}$Gd$_x$Ni$_2$B$_2$C	0.5	2.035(7)	$\approx$0.3	15.9	10(4)	11(1)
Y$_{1-x}$Gd$_x$Ni$_2$B$_2$C	2.1	2.03(3)	$\approx$0.9	14.6	9(3)	10(1)
La$_{1-x}$Gd$_x$Sn$_3$	0.4	2.010(10)	$\approx$0.5	6.4	20(2)	$\approx$20(2)

theoretical and experimental reports have shown that there is no effective doping in this class of materials[6,8] and that the suppression of T_{SDW} is given by structural parameters[7,11]. As such, in the absence of pair-breaking effects, a given structural change would lead to the same suppression of the SDW state (and the consequent emergence of SC), independent on the particular transition metal substitution. We will return to this assumption below.

With these assumptions, we can thus estimate the magnetic pair-breaking impurity potential $\langle J^2(\mathbf{q})\rangle_{AG}$ that would be necessary to cause the observed suppression of T_c for three different samples, namely, BaFe$_{1.9}$Cu$_{0.1}$As$_2$, BaFe$_{1.88}$Mn$_{0.12}$As$_2$, and the mixed doping BaFe$_{1.895}$Co$_{0.100}$Mn$_{0.005}$As$_2$ compounds. The results are shown in Table I, and reveal a remarkable disagreement (of two orders of magnitude) between $\langle J^2(\mathbf{q})\rangle_{AG}$ and the experimentally measured $\langle J^2(\mathbf{q})\rangle_{ESR}$. This is in sharp contrast to the borocarbide multi-band compounds Lu$_{1-x}$Gd$_x$Ni$_2$B$_2$C and Y$_{1-x}$Gd$_x$Ni$_2$B$_2$C, as well as to La$_{1-x}$Gd$_x$Sn$_3$, all of which display conventional pairing symmetry. For these materials, as discussed in Refs. [31, 37], the calculated $\langle J^2(\mathbf{q})\rangle_{AG}$ and the $\langle J^2(\mathbf{q})\rangle_{ESR}$ extracted from ESR experiments are in very good agreement, as expected for a conventional SC. We note that in these compounds, because of the presence of rare earth elements, one needs to properly rewrite the Abrikosov-Gor'kov Equation 1 by replacing $S(S+1)$ for $(g_J-1)^2 J(J+1)$, where $J = S + L$ is the total spin.

The huge difference between $\langle J^2(\mathbf{q})\rangle_{AG}$ and $\langle J^2(\mathbf{q})\rangle_{ESR}$ is clearly robust against small variations of $T_{c,0}$ and $\eta(E_F)$. As explained above, these conclusions rely on the assumptions that (i) the Abrikosov-Gor'kov formalism is valid and (ii) similar normal-state phase diagrams should give similar superconducting transition temperatures. To shed light on these possible issues, we also present in Table I the results for the mixed doping BaFe$_{1.895}$Co$_{0.100}$Mn$_{0.005}$As$_2$ compound[15]. The very small Mn concentration makes the AG formalism more reliable, and the fact that the compound without Mn substitution displays a superconducting transition temperature of 26 K directly determines $T_{c,0} = 26$ K. As shown in the Table, both $\langle J^2(\mathbf{q})\rangle_{AG}$ and $\langle J^2(\mathbf{q})\rangle_{ESR}$ values are very close to those of the BaFe$_{1.9}$Cu$_{0.1}$As$_2$ and BaFe$_{1.88}$Mn$_{0.12}$As$_2$ samples, displaying a deviation of two orders of magnitude.

Our findings have important consequences for the understanding of the superconductivity in the Fe-pnictides. The fact that $\langle J^2(\mathbf{q})\rangle_{ESR} \ll \langle J^2(\mathbf{q})\rangle_{AG}$ implies that the Abrikosov-Gor'kov magnetic IPB alone cannot account for the suppression of T_c. The latter must therefore be related to an unconventional magnetic IPB which must be strongly associated with the local Cu^{2+} and Mn^{2+} spins. In addition, these substitutions could also present a stronger nonmagnetic IPB effect responsible for part of the observed suppression of T_c. This also favors a non-conventional sign-changing gap function over the more conventional sign-preserving one, since in the latter case the effects of nonmagnetic IPB are expected to be weak. We note that in a s_{+-} superconductor, non-magnetic pair-breaking can be weak dependent on the ratio between intra and inter-band scattering[25,56]. Furthermore, it is also possible that the substitution of $M =$ Cu, Mn affects directly the pairing interaction, besides promoting pair-breaking. Interestingly, for $M =$ Mn substitution, along with the usual SDW-type fluctuations, Néel-type fluctuations are also

observed by inelastic neutron scattering[57]. Even when these Néel fluctuations are weak and short-ranged, they have been shown theoretically to strongly suppress T_c[58]. We note that our results are in agreement with recent measurements on LiFeAs employing angle resolved photoemission spectroscopy (ARPES) combined with quasiparticle interference (QPI) by means of scanning tunneling microscopy/spectroscopy (STM/STS)[59].

Finally, we comment on the effects of pressure on T_c, summarized in Fig. 4. For the Co and Ni substitutions, the rate dT_c/dP is $\sim$0.1 K/kbar and the application of pressure has little effect on T_c. Strikingly, this rate is three times larger for the $M =$ Cu sample, while for $M =$ Mn, no SC is observed. We argue that these results are linked to the magnetic pair-breaking discussed above. In particular, because pressure increases the hybridization between the Cu 3d bands and conduction electron bands, the copper bands become more itinerant, progressively losing their local moment character and consequently suppressing the magnetic IPB effect. Therefore, it is not surprising that the pure BaCu$_2$As$_2$ is a Pauli paramagnet with completely delocalized Cu 3d bands and no phase transition. Within this scenario, the fact that the Mn compounds do not display SC would follow from the fact that Mn^{2+} has a spin value five times larger than Cu^{2+}. Interestingly, if the magnetic IPB mechanism is suppressed by pressure, T_c is, in principle, unconstrained to increase up to a maximum defined by the local distortions that the M-substitution creates. For Cu-substituted samples, it remains to be confirmed whether applying higher pressures with Diamond Anvil Pressure cells would further enhance or even suppress T_c in the impurity pair-breaking regime.

To make this reasoning more quantitative, we assume that the enhancement of T_c caused by the magnetic IPB suppression with pressure follows a phenomenological expression of the form ΔT_c
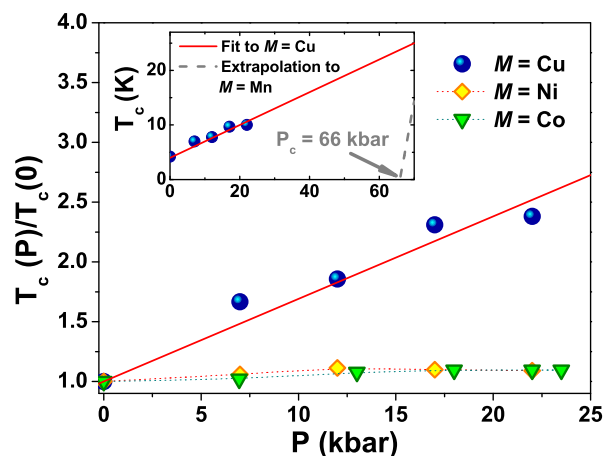

Figure 4 | Phase diagram for BaFe$_{2-x}$M$_x$As$_2$ ($M =$ Co, Cu, and Ni) single crystals as a function of pressure. The dotted lines are guide to the eyes for the SC domes. The linear fit for the $M =$ Cu compound (solid line) was obtained from the phenomenological expression $\Delta T_c = S(S+1)(a - bP)$. Using the same expression and $S = 5/2$, we obtain the dashed line for the $M =$ Mn compound.

$= S(S + 1)(a − bP)$, where a and b are free parameters and P, applied pressure. The linear dependence with pressure is motivated by the same typical dependence of the Kondo temperature (T_K) on pressure in several Ce-based heavy fermion compounds[43–47]. This linear regime can be applied to the M = Cu (S = 1/2) compound in the IPB region slightly below the optimally-doped concentration, where the spin fluctuactions are nearly constant as a function of pressure. This procedure allows one to obtain the linear fit to the experimental data (solid line) displayed in Fig. 4. On the other hand, for M = Cu compounds in the optimally-doped or overdoped regions, the spin fluctuation suppression starts to play an important role and would overcome the latter linear increase of T_c. A detailed study on the effects of Cu substitution in critical current measurements is presented in Ref. [14]. Now, by constraining the same linear dependence for M = Mn and changing only the spin value to S = 5/2, we obtain a lower limit for the critical pressure $P_c \sim 66$ kbar necessary for the emergence of SC (dashed line in Fig. 4). This P_c value is in good agreement with the experimental absence of SC in the M = Mn compounds up to 25 kbar (see Fig. 2d), also in agreement with previous reports[16].

In conclusion, we have demonstrated the contrasting behavior of hydrostatic pressure effects on nearly OPD BaFe$_{2−x}$M$_x$As$_2$ (M = Co, Cu, and Ni) high-quality single crystals grown from In-flux method. The striking enhancement of T_c with pressure for M = Cu and the existence of a Cu^{2+} ESR line provide strong evidence of a spin-dependent pair-breaking mechanism strongly suppressed by pressure, suggesting an increase of hybridization between the Cu $3d$ bands and the conduction electron bands. More interestingly, by using the magnetic impurity potential extracted from the ESR analysis in the absence of *bottleneck* effects, we find that the Abrikosov-Gor'kov pair-breaking mechanism, applied to a conventional sign-preserving pairing state, cannot account for the observed suppression of T_c in the Cu and Mn-substituted compounds. This result not only implies that the suppression of T_c in these samples is due to other mechanisms, but also that an unconventional pairing state is more likely to be realized.

Methods

Single crystals of BaFe$_{1.9}$M$_{0.1}$As$_2$ (M = Mn, Co, Cu, and Ni) were grown using In-flux as described elsewhere[39]. The crystals were checked by x-ray powder diffraction and submitted to elemental analysis using a commercial EDS microprobe. In-plane electrical resistivity measurements were performed using a standard four-probe method and a self-contained piston-cylinder type Be-Cu pressure cell, with a core of hardened NiCrAl alloy. ESR spectra were taken in a commercial ELEXSYS 500 X-band (v = 9.5 GHz) spectrometer equipped with a continuous He gas-flow cryostat.

1. Kamihara, Y., Watanabe, T., Hirano, M. & Hosono, H. Iron-based layered superconductor La[O$_{1−x}$F$_x$]FeAs (x = 0.05–0.12) with T_c = 26 K. *J. Am. Chem. Soc.* **130**, 3296 (2008).

2. Rotter, M. *et al.* Spin density wave anomaly at 140 K in the ternary iron arsenide BaFe$_2$As$_2$. *Phys. Rev. B* **78**, 020503(R) (2008).

3. Ishida, K., Nakai, Y. & Hosono, H. To What Extent Iron-Pnictide New Superconductors Have been Clarified: A Progress Report. *J. Phys. Soc. Japan* **78**, 062001 (2009).

4. Hirschfeld, P. J., Korshunov, M. M. & Mazin, I. I. Gap symmetry and structure of Fe-based superconductors. *Rep. Prog. Phys.* **74**, 124508 (2011).

5. Chubukov, A. V. Pairing Mechanism in Fe-Based Superconductors. *Annu. Rev. Cond. Mat. Phys.* **3**, 57 (2012).

6. Bittar, E. M. *et al.* Co-Substitution Effects on the Fe Valence in the BaFe$_2$As$_2$ Superconducting Compound: A Study of Hard X-Ray Absorption Spectroscopy. *Phys. Rev. Lett.* **107**, 267402 (2011).

7. Granado, E. *et al.* Pressure and chemical substitution effects in the local atomic structure of BaFe$_2$As$_2$. *Phys. Rev. B* **83**, 184508 (2011).

8. Wadati, H., Elfimov, I. & Sawatzky, G. A. Where Are the Extra d Electrons in Transition-Metal-Substituted Iron Pnictides? *Phys. Rev. Lett.* **105**, 157004 (2010).

9. Ideta, S. *et al.* Dependence of Carrier Doping on the Impurity Potential in Transition-Metal-Substituted FeAs-Based Superconductors. *Phys. Rev. Lett.* **110**, 107007 (2013).

10. Berlijn, T., Lin, C.-H., Garber, W. & Ku, W. Do Transition-Metal Substitutions Dope Carriers in Iron-Based Superconductors? *Phys. Rev. Lett.* **108**, 207003 (2012).

11. Hin, Z. P., Haule, K. & Kotliar, G. Kinetic frustration and the nature of the magnetic and paramagnetic states in iron pnictides and iron chalcogenides. *Nature Materials* **10**, 932â935 (2011).

12. Rosa, P. F. S. *et al.* Evolution of Eu^{2+} spin dynamics in Ba$_{1−x}$Eu$_x$Fe$_2$As$_2$. *Phys. Rev. B* **86**, 165131 (2012).

13. Rosa, P. F. S. *et al.* Site specific spin dynamics in BaFe$_2$As$_2$: tuning the ground state by orbital differentiation. arxiv:1402.2001v01 (2014).

14. Garitezi, T. M. *et al.* Transport critical current measurements on a Cu-substituted BaFe$_2$As$_2$ superconductor. *J. Appl. Phys.* **115**, 17D704 (2014).

15. Rosa, P. F. S. *et al.* Pressure effects on magnetic pair-breaking in Mn- and Eu-substituted BaFe$_2$As$_2$. *J. Appl. Phys.* **115**, 17D702 (2014).

16. Thaler, A. *et al.* Physical and magnetic properties of Ba(Fe$_{1−x}$Mn$_{x}$)$_2$As$_2$ single crystals. *Phys. Rev. B* **84**, 144528 (2011).

17. Ahilan *et al.* Pressure effects on the electron-doped high T_c superconductor BaFe$_{2−x}$Co$_x$As$_2$. *J Phys. Cond. Mat.* **20**, 472201 (2008).

18. Drotziger *et al.* Pressure versus concentration tuning of the superconductivity in Ba(Fe$_{1−x}$Co$_x$)$_2$As$_2$. *J. Phys. Soc. Japan* **79**, 124705 (2010).

19. Yamaichi, S., Katagiri, T. & Sasagawa, T. Uniaxial pressure effects on the transport properties in Ba(Fe$_{1−x}$Co$_x$)$_2$As$_2$ single crystals. *Physica C* **494**, 62–64 (2013).

20. Canfield, P. C., Bud'ko, S. L., Ni, N., Yan, J. Q. & Kracher, A. Decoupling of the superconducting and magnetic/structural phase transitions in electron-doped BaFe$_2$As$_2$. *Phys. Rev. B* **80**, 060501(R) (2009).

21. Kirshenbaum, K., Saha, S. R., Ziemak, S., Drye, T. & Paglione, J. Universal pair-breaking in transition metal-substituted iron-pnictide superconductors. *Phys. Rev. B* **86**, 140505(R) (2012).

22. Onari, S. & Kontani, H. Violation of Andersonâs Theorem for the Sign-Reversing s-Wave State of Iron-Pnictide Superconductors. *Phys. Rev. Lett.* **103**, 177001 (2009).

23. Li, J. *et al.* Superconductivity suppression of Ba$_{0.5}$K$_{0.5}$Fe$_{2−2x}$Mn$_{2x}$As$_2$ single crystals by substitution of transition metal (M = Mn, Ru, Co, Ni, Cu, and Zn). *Phys. Rev. B*, **85**, 214509 (2012).

24. Bang, Y., Choi, H.-Y. & Won, H. Impurity effects on the $s_\pm$-wave state of the iron-based superconductors. *Phys. Rev. B* **79**, 054529 (2009).

25. Wang, Y., Kreisel, A., Hirschfeld, P. J. & Mishra, V. Using controlled disorder to distinguish $s_\pm$ and s_{++} gap structure in Fe-based superconductors. *Phys. Rev. B* **87**, 094504 (2013).

26. Fernandes, R. M., Vavilov, M. G. & Chubukov, A. V. Enhancement of T_c by disorder in underdoped iron pnictide superconductors. *Phys. Rev. B* **85**, 140512(R) (2012).

27. Ni, N. *et al.* Temperature versus doping phase diagrams for Ba(Fe$_{1−x}$TM$_x$)$_2$As$_2$ (TM = Ni,Cu,Cu/Co) single crystals. *Phys. Rev. B* **82**, 024519 (2010).

28. Patz, A. *et al.* Ultrafast observation of critical nematic fluctuations and giant magnetoelastic coupling in iron pnictides. *Nature Comm.* **5**, 3229 (2014).

29. Abrikosov, A. A. & Gor'kov, L. P. Contribution to the theory of superconducting alloys with paramagnetic impurities. *Sov. Phys. JETP* **12**, 1243 (1961).

30. Skalski, S., Betbeder-Matibet, O. & Weiss, P. R. Properties of Superconducting Alloys Containing Paramagnetic Impurities. *Phys. Rev.* **136**, A1500–A1518 (1964).

31. Pagliuso, P. G. *et al.* Electron spin resonance of Gd^{3+} in the normal state of RNi$_2$B$_2$C (R = Y, Lu). *Phys. Rev. B* **57**, 3668 (1998).

32. Korringa, J. Nuclear magnetic relaxation and resonance line shift in metals. *Physica* **16**, 601 (1950).

33. Rettori, C. *et al.* Dynamic behavior of paramagnetic ions and conduction electrons in intermetallic compounds: Gd$_x$Lu$_{1−x}$Al$_2$. *Phys. Rev. B* **10**, 1826 (1974).

34. Davidov, D. *et al.* Electron spin resonance of Gd in the intermetallic compounds YCu, YAg, and LaAg: Wave vector dependence of the exchange interaction. *Solid State Comm.* **12**, 621 (1973).

35. Narath, A. & Weaver, H. T. Effects of Electron-Electron Interactions on Nuclear Spin-Lattice Relaxation Rates and Knight Shifts in Alkali and Noble Metals. *Phys. Rev.* **175**, 373 (1968).

36. Shaw, R. W. & Warren, W. W. Enhancement of the Korringa Constant in Alkali Metals by Electron-Electron Interactions. *Phys. Rev. B* **3**, 1562 (1971).

37. Bittar, E. M. *et al.* Electron spin resonance study of the LaIn$_{3−x}$Sn$_x$ superconducting system. *J. of Phys.: Cond. Matt.* **23**, 455701 (2011).

38. Maple, M. B. Dependence of $s − f$ exchange on atomic number in rare earth dialuminides. *Solid State Comm.* **8**(22), 1915–1917 (1970).

39. Garitezi, T. M. *et al.* Synthesis and Characterization of BaFe$_2$As$_2$ Single Crystals Grown by In-flux Technique. *Brazilian Journal of Physics* **43**, 223 (2013).

40. Alireza, P. L. *et al.* Superconductivity up to 29 K in SrFe$_2$As$_2$ and BaFe$_2$As$_2$ at high pressures. *J. Phys.: Condens. Matter* **21**, 012208 (2009).

41. Rotter, M., Tegel, M. & Johrendt, D. Superconductivity at 38 K in the Iron Arsenide Ba$_{1−x}$K$_x$Fe$_2$As$_2$. *Phys. Rev. Lett.* **101**, 107006 (2008).

42. Wang, C. *et al.* Thorium-dopingâinduced superconductivity up to 56âK in Gd$_{1−x}$Th$_x$FeAsO. *EPL* **83**, 67006 (2008).

43. Shibata, A. *et al.* Thorium-dopingâinduced superconductivity up to 56âK in Gd$_{1−x}$Th$_x$FeAsO. *J. Phys. Soc. Jpn.* **55**, 6 (1986).

44. Cooley, J. C., Aronson, M. C. & Canfield, P. C. High pressures and the Kondo gap in Ce$_3$Bi$_4$Pt$_3$. *Phys. Rev. B* **55**, 7533 (1997).

45. Oomi, G. & Kagayama, T. Effect of pressure and magnetic field on the electrical resistivity of cerium kondo compounds. *J. Phys. Soc. Jpn.* **65** Suppl. B 42–48 (1996).

46. Ramos, S. M. *et al.* Superconducting Quantum Critical Point in CeCoIn$_{5-x}$Sn$_x$. *Phys. Rev. Lett.* **105**, 126401 (2010).
47. Hering, E. N. *et al.* Pressure–temperature–composition phase diagram of Ce$_2$MIn$_8$. *Physica B: Cond. Matt.* **378** (2006).
48. Dyson, F. J. Electron Spin Resonance Absorption in Metals. II. Theory of Electron Diffusion and the Skin Effect. *Phys. Rev.* **98**, 349 (1955).
49. Texier, Y. *et al.* Mn local moments prevent superconductivity in iron pnictides Ba(Fe$_{1-x}$Mn$_x$)$_2$As$_2$. *EPL* **99**, 17002 (2012).
50. LeBoeuf, D. *et al.* NMR study of electronic correlations in Mn-doped Ba(Fe$_{1-x}$Co$_x$)$_2$As$_2$ and BaFe(As$_{1-x}$P$_x$)$_2$. *arXiv1310.4969* (2013).
51. Suzuki, H. *et al.* Absence of superconductivity in the hole-doped Fe pnictide Ba(Fe$_{1-x}$Mn$_x$)$_2$As$_2$: Photoemission and x-ray absorption spectroscopy studies. *Phys. Rev. B* **88**, 100501(R) (2013).
52. Kim, M. G. *et al.* Effects of Transition Metal Substitutions on the Incommensurability and Spin Fluctuations in BaFe$_2$As$_2$ by Elastic and Inelastic Neutron Scattering. *Phys. Rev. Lett.* **109**, 167003 (2012).
53. Frankovsky *et al.* Short-range magnetic order and effective suppression of superconductivity by manganese doping in LaFe$_{1-x}$Mn$_x$AsO$_{1-y}$F$_y$. *Phys. Rev. B* **87**, 174515 (2013).
54. Golubov, A. A. & Mazin, I. I. Effect of magnetic and nonmagnetic impurities on highly anisotropic superconductivity. *Phys. Rev. B* **55**, 15146 (1997).
55. Openov, L. A. Combined effect of nonmagnetic and magnetic scatterers on the critical temperatures of superconductors with different anisotropies of the gap. *JETP Lett.* **66**, 661 (1997).
56. Efremov, D. V. *et al.* Disorder-induced transition between $s_\pm$ and s_{++} states in two-band superconductors. *Phys. Rev. B* **84**, 180512(R) (2011).
57. Tucker, G. S. *et al.* Competition between stripe and checkerboard magnetic instabilities in Mn-doped BaFe$_2$As$_2$. *Phys. Rev. B* **86**, 020503(R) (2012).
58. Fernandes, R. M. & Millis, A. J. Suppression of Superconductivity by Neel-Type Magnetic Fluctuations in the Iron Pnictides. *Phys. Rev. Lett.* **110**, 117004 (2013).
59. Chi, S. *et al.* Sign inversion in the superconducting order parameter of LiFeAs inferred from Bogoliubov quasiparticle interference. arXiv:1308.4413v1 (2013).
60. Johnston, D. C. *Adv. Phys.* **59**, 803 (2010); Paglione, J. & Greene, R. L. High-temperature superconductivity in iron-based materials. *Nature Phys.* **6**, 645 (2010).
61. Wen, H. H. & Li, S. Materials and Novel Superconductivity in Iron Pnictide Superconductors. *Annu. Rev. Cond. Mat. Phys.* **2**, 121 (2011)
62. Stewart, G. R. Superconductivity in Iron Compounds. *Rev. Mod. Phys.* **83**, 1589–1652 (2011).

Acknowledgments

Author contributions

P.F.S.R., C.A. and T.M.G. have grown the single crystals and performed pressure dependent transport measurements. P.F.S.R. performed ESR measurements. T.G. performed EDS measurements. R.M.F. performed theoretical analyses. P.F.S.R., C.A., T.M.G., T.G., Z.F., R.R.U., R.M.F. and P.G.P. discussed the data and reviewed the manuscript.

Additional information